REPORT SSD-TR-89-66

AD-A213 730

(4)

Development of the RAIDS Extreme Ultraviolet Wedge and Strip Detector

Prepared by

D. C. KAYSER, W. T. CHATER, A. B. CHRISTENSEN,
C. K. HOWEY, and J. B. PRANKE
Space Sciences Laboratory
The Aerospace Corporation
El Segundo, CA 90245

and

S. CHAKRABARTI and O. H. W. SIEGMUND
Space Sciences Laboratory
University of California, Berkeley, CA 94720

28 August 1989

Prepared for

SPACE SYSTEMS DIVISION
AIR FORCE SYSTEMS COMMAND
Los Angeles Air Force Base
P.O. Box 92960
Los Angeles, CA 90009-2960

This report was submitted by The Aerospace Corporation, El Segundo, CA 90245, under Contract No. F04701-88-C-0089 with the Space Systems Division, P.O. Box 92960, Los Angeles, CA 90009-2960. It was reviewed and approved for The Aerospace Corporation by H. R. Rugge, Director, Space Sciences Laboratory. Capt Leslie Belsma was the project officer for the Mission-Oriented Investigation and Experimentation (MOIE) Program.

This report has been reviewed by the Public Affairs Office (PAS) and is releasable to the National Technical Information Service (NTIS). At NTIS, it will be available to the general public, including foreign nationals.

This technical report has been reviewed and is approved for publication. Publication of this report does not constitute Air Force approval of the report's findings or conclusions. It is published only for the exchange and stimulation of ideas.

Leslie O Belsma

LESLIE BELSMA, CAPT, USAF
MOIE Project Officer
SSD/DAAX

Raymond M Leong

RAYMOND M. LEONG, MAJOR, USAF
MOIE Program Manager
AFSTC/WCO OL-AB

UNCLASSIFIED

SECURITY CLASSIFICATION OF THIS PAGE

REPORT DOCUMENTATION PAGE

1a. REPORT SECURITY CLASSIFICATION Unclassified	1b. RESTRICTIVE MARKINGS
2a. SECURITY CLASSIFICATION AUTHORITY	3. DISTRIBUTION/AVAILABILITY OF REPORT Approved for public release; distribution unlimited
2b. DECLASSIFICATION/DOWNGRADING SCHEDULE	
4. PERFORMING ORGANIZATION REPORT NUMBER(S) TR-0088(3940-04)-2	5. MONITORING ORGANIZATION REPORT NUMBER(S) SSD-TR-89-66
6a. NAME OF PERFORMING ORGANIZATION The Aerospace Corporation Laboratory Operations 6b. OFFICE SYMBOL *(If applicable)*	7a. NAME OF MONITORING ORGANIZATION Space Systems Division
6c. ADDRESS *(City, State, and ZIP Code)* El Segundo, CA 90245	7b. ADDRESS *(City, State, and ZIP Code)* Los Angeles Air Force Base Los Angeles, CA 90009-2960
8a. NAME OF FUNDING/SPONSORING ORGANIZATION 8b. OFFICE SYMBOL *(If applicable)*	9. PROCUREMENT INSTRUMENT IDENTIFICATION NUMBER F04701-85-C-0086-P00019
8c. ADDRESS *(City, State, and ZIP Code)*	10. SOURCE OF FUNDING NUMBERS PROGRAM ELEMENT NO. / PROJECT NO. / TASK NO. / WORK UNIT ACCESSION NO.

11. TITLE *(Include Security Classification)*
Development of the RAIDS Extreme Ultraviolet Wedge and Strip Detector

12. PERSONAL AUTHOR(S) Kayser, D. C., Chater, W. T., Christensen, A. B., Howey, C. K., and Pranke, J. B., (The Aerospace Corporation) Chakrabarti, S. and Siegmund, O. H. M., (University of California)

13a. TYPE OF REPORT	13b. TIME COVERED	14. DATE OF REPORT *(Year, Month, Day)*	15. PAGE COUNT
	FROM _____ TO _____	1989 August 28	15

16. SUPPLEMENTARY NOTATION

17. COSATI CODES			18. SUBJECT TERMS *(Continue on reverse if necessary and identify by block number)*
FIELD	GROUP	SUB-GROUP	Alumina Kovar

19. ABSTRACT *(Continue on reverse if necessary and identify by block number)*

In the next few years the Remote Atmospheric and Ionospheric Detector System (RAIDS) package will be flown on a TIROS spacecraft. The Extreme Ultraviolet Spectrometer (EUVS) experiment contains a position-sensitive detector based on wedge and strip anode technology. A University of California Berkeley detector design has been implemented in brazed alumina and kovar to provide a rugged bakeable housing and anode. A stack of three 80:1 microchannel plates is operated at 3500–4100 V to achieve a gain of $\geq 10^7$. The top MCP is to be coated with MgF for increased quantum efficiency in the range of 500–1150 A. Fabrication of the wedge and strip anode on brazed alumina has presented some challenging problems. In this report, a summary of fabrication techniques and detector performance characteristics is presented.

20. DISTRIBUTION/AVAILABILITY OF ABSTRACT	21. ABSTRACT SECURITY CLASSIFICATION	
[X] UNCLASSIFIED/UNLIMITED [ ] SAME AS RPT. [ ] DTIC USERS	Unclassified	
22a. NAME OF RESPONSIBLE INDIVIDUAL	22b. TELEPHONE *(Include Area Code)*	22c. OFFICE SYMBOL

DD FORM 1473, 84 MAR — 83 APR edition may be used until exhausted. All other editions are obsolete

SECURITY CLASSIFICATION OF THIS PAGE

UNCLASSIFIED

PREFACE

This work was supported by the U. S. Air Force Systems Command's Space Systems Division under Contract No. F04701-85-C-0086-P00019 and by NASA under grant NSG-6032.

CONTENTS

I. INTRODUCTION 7

II. PHYSICAL APPEARANCE 9

III. FABRICATION TECHNIQUES AND PROBLEMS 11

IV. HIGH VOLTAGE AND POLARITY CONSIDERATIONS 15

V. DIELECTRIC EFFECTS OF ALUMINA 17

VI. SUMMARY AND CONCLUSIONS 19

REFERENCES 20

FIGURES

1. The EUVS Detector Showing Component Parts 9
2. Detail of Wedge and Strip Pattern Metallized in Gold on an Alumina Substrate . 10
3. A Schematic Drawing of the Detector High Voltage Bias Network 15

TABLES

I. Typical Grades of Alumina and Their Crystal Size 12

II. Inter-Electrode Capacitances for Wedge and Strip Patterns on Alumina and Quartz 17

I. INTRODUCTION

The eight instruments of the RAIDS experiment have been previously described.[1] One of these, the EUVS, is intended to measure emissions in the spectral range of 500–1150 Å. In order to maximize instrumental sensitivity at these wavelengths, the design calls for a wedge and strip anode type detector using three 80:1 microchannel plates for signal multiplication. The top microchannel plate is to be coated with MgF for improved quantum efficiency. With an overall dark count rate of 2–3 counts per second, the wedge and strip design provides a favorable signal-to-noise ratio at the moderate count rates (100–8000 s^{-1}) which are typical in this wavelength range.

A sealed, windowed detecto is infeasible due to the lack of transmitting materials in the spectral range of 500–1150 Å. For cleanliness and stability we have designed a windowless detector which uses a vacuum-tight moveable entrance door. The door can be opened for instrumental ground testing and calibration, and is permanently deployed for measurements in orbit. In order to achieve overall ruggedness it was decided to implement the University of California Berkley wedge and strip design on an alumina substrate which, in turn, is monolithic with the detector shell.

II. PHYSICAL APPEARANCE

Figure 1 is a photograph which shows the mechanical components of the wedge and strip detector assembly. The detector shell is composed of a series of kovar and alumina parts which are brazed together to form a vacuum-tight structure. The shell (in photo background) is shown both with (right) and without (middle) the front vacuum door flange. This flange is sealed to the shell by means of a compressible gold gasket. In the left photo background is the wedge and strip anode which will be discussed later. The set of small parts (foreground semi-circle) along with a stack of three microchannel plates is inserted from the top of the shell to form the multiplier section of the detector.

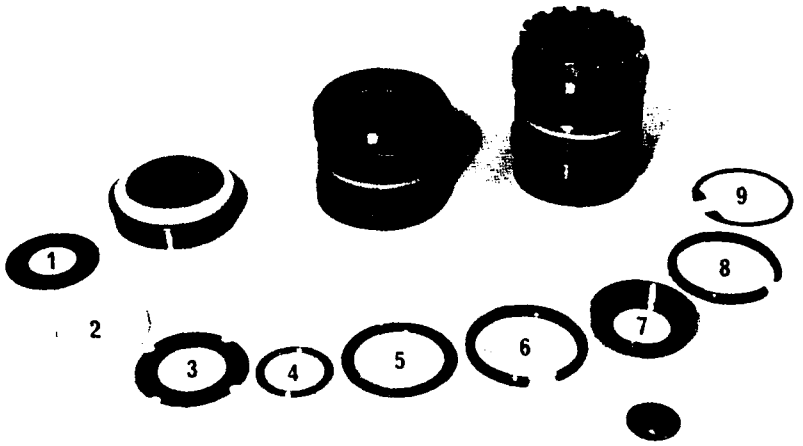

Fig. 1. The EUVS Detector Showing Component Parts. The microchannel plates are not shown here.

Proceeding left to right in sequence, the assembly goes as follows: Three microchannel plates (not shown) rest on the flat plate bed (1) and are surrounded by the ceramic washer (2). The flat, tempered copper gasket (3) presses on the pressure pad (4) which in turn rests on top of the microchannel plates. The spring press (5) is constrained by the spring clip (6), and rests on and deforms the copper gasket, thereby compressing the stack of microchannel plates. The screen frame (7) rests on the next spring clip (8) and holds a high-transmission repeller grid (not visible). The screen frame is constrainted by the spring ring (9). The use of spring clips ensures mechanical stability of the parts stack and also allows disassembly of the unit. Electrical connections for the high-voltage bias network are made by spot welding solder tabs to the kovar rings of the shell.

Figure 2 shows the wedge and strip anode in greater detail. The metallized pattern has been created directly on an alumina substrate which was previously brazed to the kovar anode structure. The metal layer of the pattern consists of 2 μm of gold deposited over ~400 Å of W/Ti. The W/Ti layer ensures quality bonding of the pattern to the substrate. Electrical connections to the pattern are provided by four kovar pins which are brazed through the substrate to the opposite side of the anode. The metallizing process deposits the leads of the wedge and strip pattern directly over the braze pads which surround the kovar pins at the surface of the substrate. Prior to final assembly of a detector the anode is beam welded to the detector shell to provide vacuum integrity. The result is a monolithic structure without stand-offs or screws which should easily withstand vibration.

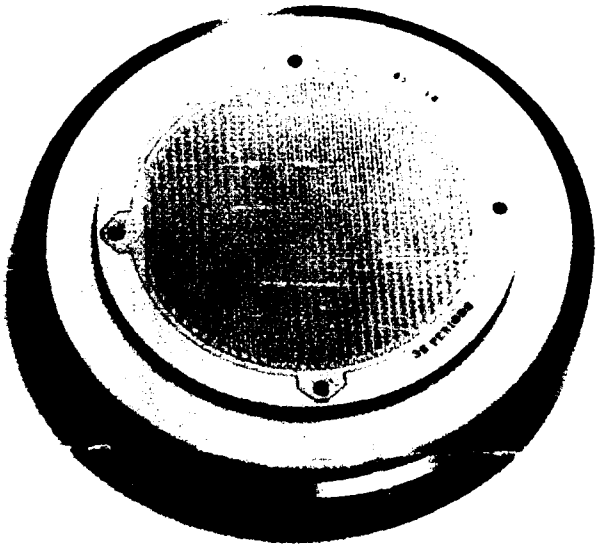

Fig. 2. Detail of the Wedge and Strip Pattern Metallized in Gold on an Alumina Substrate.

III. FABRICATION TECHNIQUES AND PROBLEMS

Fabrication of the alumina and kovar assemblies was relatively uneventful. Ordinarily, alumina parts are machined from finished alumina stock, but machining costs are high due to the hardness of the material. For this reason we engaged R&W Products, Inc. of Auburn, CA which machines oversized alumina parts in a "green" state. After shrinkage during firing, the parts become finished alumina of the required size and shape, ready for brazing. R&W Products also provided the required brazing services. With their expertise we have fabricated several shells with sufficient vacuum integrity. Alignment and concentricity requirements are critical due to the ring structure used for the internal parts. For this reason we might in the future reduce the thickness of the kovar parts to minimize internal strains in the finished shells.

The first indication of substantial difficulty came when UC Berkeley attempted to metallize the brazed anode assemblies. Previously the Berkeley group had routinely produced copper patterns on a quartz substrate.[2] We anticipated a smooth transfer of this technology with the substitution of alumina. In fact, the attempt did not work. Achieving a suitable surface polish on the substrate was difficult, if not impossible. When the deposited copper layer was etched, residual copper remained in numerous imperfections on the surface and a bulk short among the anode elements resulted. Metallizing of several pieces was tried, and each piece exhibited this problem to varying degrees. We did not know it at the time but we had begun a two-year odyssey which led finally to the finished anode of Fig. 2.

Suspecting surface imperfections due to the use of the "green" process, we explored the possibility of glazing the substrate. The problem with this approach is to find a high temperature glaze that is unaffected by subsequent brazing cycles or a very low temperature glaze that can be applied after brazing. The former approach was tried but led to crazing of the surface. A second suspicion was that temperature cycling during brazing might be modifying the crystal domains of the substrate. Subsequent polishing might then lead to larger "pullouts" or pits.

Two parallel efforts were undertaken. In the first we engaged the Coors Ceramic Company of Golden, CO to produce a machined alumina substrate which would be brazed as before. We specified that some samples were to be run through a brazing temperature cycle to simulate brazing effects. In the second effort we obtained the services of The Aerospace Corporation Electronics Research Laboratory to attempt some masking and metallizing procedures that are normally used in the production of microelectronic circuits. It was thought that with these techniques we might be able to mitigate the effect of surface imperfections. In fact, this latter effort did not lead to any clearly better approaches.

A second set of anodes was brazed using the new machined alumina substrates. Substrate samples which had been run through the simulated brazing cycles showed no obvious differences from untreated samples. With the goal of achieving high durablity in the fin-

ished product, we engaged Engelhard Corp. of Millis, MA to metallize the anodes in gold with a bonding layer of W/Ti. In their first attempt at metalization, Engelhard reported, as Berkeley had before them, that bulk shorts remained after a standard metallizing and etching process. In subsequent attempts they have been able to modify their procedure sufficiently to produce a limited number of functional anodes. Because of the extensive reprocessing required, neither they nor we consider the present situation satisfactory. After discussions with a number of knowledgeable people in the ceramics business, we have concluded that the ceramics industry typically supports three distinct technologies: One technology requires brazeable alumina such as we have used in our shell assemblies. These ceramics support high-strength, high-temperature brazing, but in this application surface finish is a secondary consideration. The second technology is typically microelectronic oriented, and requires small wafers of high purity alumina which are polished and bonded into assemblies with specialized brazes. The third technology is food-service oriented. In this application, surface finish of the alumina is important, but no brazing is required.

Our problem is that we are seeking both superior polish and braze qualities from the same material. As a specific example, Table I lists typical grades of alumina available from Coors along with corresponding average crystal sizes in micrometers. According to brazing vendors, brazable grades of alumina fall in the range of 94–97% purity. A glass content of 3 to 6% is required to provide strong bonding between the alumina and the metallization layer. Conversely, polishing tends to remove the glass component at the surface, thus producing larger voids with decreasing purity of the alumina. Although crystal size tends to increase with purity, as is illustrated in Table I, special processing can produce small crystal

Table I. Typical Grades of Alumina and Their Crystal Size[+]

Grade Designation	Crystal Size (μm)	% alumina
AD-85	6	85.0
AD-90	4	90.0
AD-94	12	94.0
AD-96	11	96.0
AD-995	17	99.5
AD-997 (K-5)	3	99.7
VISTAL	20	99.9

[+] From Coors Ceramics Company brochure

size in a high-purity alumina. This is evidenced in the K-5 material of 99.7% purity with 3 μm average crystal size. In our application the surface characteristics of K-5 would be ideal. However, in keeping with the conventional wisdom, a sample of K-5 test-brazed to kovar yielded a joint with only 20% of the normal pull strength. In future anode designs we may be able to accomodate weaker braze joints typical of K-5, or we may resort to a metallized sandwich wherein both types of ceramic can be incorporated in a complementary fashion.

IV. HIGH VOLTAGE AND POLARITY CONSIDERATIONS

Conventional operation of the wedge and strip detector is obtained with the anode at signal ground and the cathode at negative high voltage. The present detector biasing scheme for EUVS puts the cathode at nominal ground and the wedge and strip anode at positive high voltage (Fig. 3). This scheme was adopted to minimize the effects of a large flux of ambient ions which would impinge on the EUVS when the instrument is pointed in the ram direction. With the photocathode at ground, ions are not attracted to the detector and hence background noise can be controlled. However, in this configuration electrical turn on and turn off transients have a more pronounced effect on the anode and impose additional durability requirements on the wedge and strip pattern.

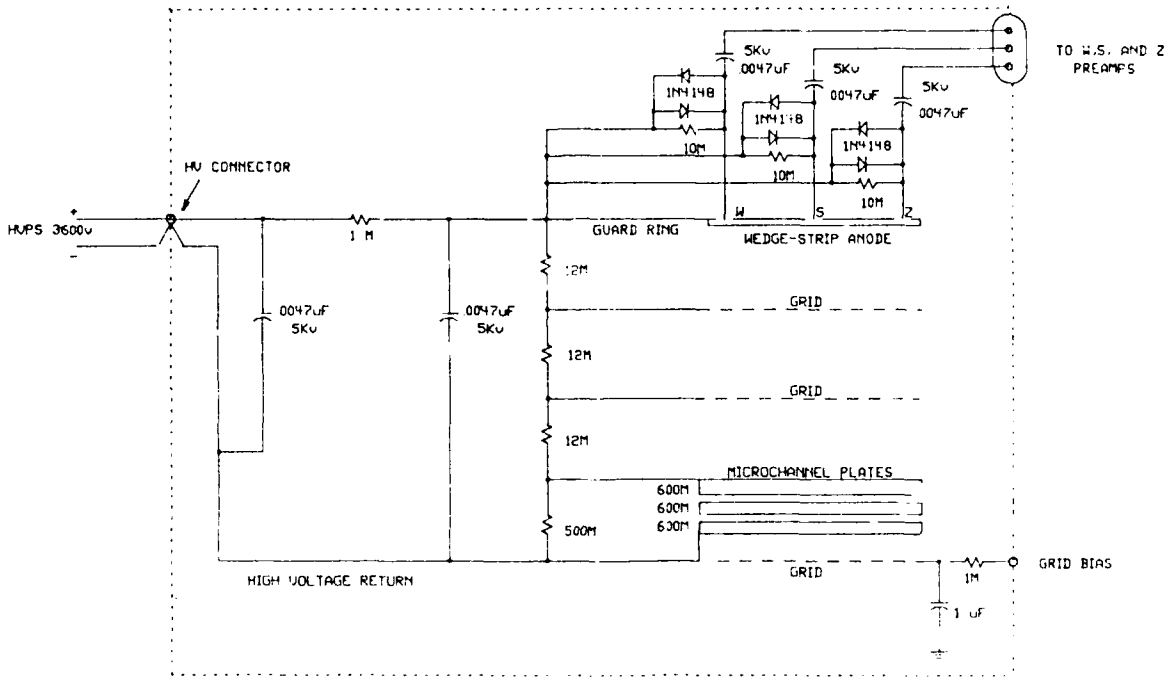

Figure 3. A Schematic Drawing of the Detector High Voltage Bias Network.

Figure 3 shows a fully protected detector bias network with high-voltage blocking capacitors for the connection of charge preamplifiers. On the left side of the figure is an RC network which is used not only to filter ripple on the high-voltage power supply but also to suppress rise time transients. Smoothing of transients is important because the W, S, and Z components of the anode pattern are charged independently through their respective 10 M

Ω resistors. Due to normal tolerances in the values of the resistors and blocking capacitors, each point follows its own charging curve. In this circumstance it is possible to develop substantial momentary voltage differences beween, say, the strip pattern and the guard ring, leading to arcing and destruction of the pattern. We have experienced this effect with copper metallized patterns and were prompted to include back-to-back protective diodes as shown in the figure. Because diodes exhibit leakage currents, it is preferrable to use unprotected anodes that are capable of surviving occasional arcs without damage. Our experience to date indicates that the new gold patterns appear to have a greater tolerance toward discharges, which raises the expectation that we may be able to fly them without diodes.

V. DIELECTRIC EFFECTS OF ALUMINA

The dielectric constants of alumina and quartz are quite different. A typical dielectric constant for quartz is 4.3 (at 1 Mhz) whereas for alumina it is 8.9. Not surprisingly, inter-electrode capacitances of the wedge and strip pattern change correspondingly. Table II shows typical values for patterns deposited on quartz and on alumina. In general, capacitances of a pattern on alumina jump by ~2.25, in line with a change in the dielectric constant of ~2.1. In systems requiring high resolution, lowered inter-electrode capacitance has been one argument for the use of quartz substrates.[2] We have not attempted a detailed study of related capacitive effects since, at the present medium operating resolution of the EUVS, such effects should be negligible.

Table II. Inter-Electrode Capacitances for Wedge and Strip Patterns on Alumina and Quartz Component Value for Alumina Value for Quartz

Component Measured	Value for Alumina (pf)	Value for Quartz (pf)
S to Z	180	79
W to Z	180	79
W to S	36	17

VI. SUMMARY AND CONCLUSIONS

In spite of the fabrication problems just outlined, we have produced a useful number of ruggedized wedge and strip detector assemblies. Whether the characteristics of these devices at the highest resolutions are comparable to devices fabricated on quartz is a question for future investigation. Higher quality anode patterns can certainly be produced once alumina with an appropriate surface finish is incorporated in the design. It should also be noted that the overall design of the brazed assembly could be improved in time through miniaturization of component parts, leading to lighter weight and increased strength.

REFERENCES

1. R. P. McCoy, K. D. Wolfram, R. R. Meier, L. J. Paxton, D. D. Cleary, D. K. Prinz, D. E. Anderson, Jr., A. B. Christensen, J. Pranke, G. G. Sivjee and D. C. Kayser, "The Remote Atmospheric and Ionospheric Detection System," SPIE Ultraviolet Technology, 687, 142–149 (1986).

2. O. H. W. Siegmund, M. Lampton, J. Bixler, S. Bowyer, and R. F. Malina, "Operational Characteristics of Wedge and Strip Image Readout Systems," IEEE Trans. Nucl. Sci. 33(1), 724–727 (1986).

LABORATORY OPERATIONS

The Aerospace Corporation functions as an "architect-engineer" for national security projects, specializing in advanced military space systems. Providing research support, the corporation's Laboratory Operations conducts experimental and theoretical investigations that focus on the application of scientific and technical advances to such systems. Vital to the success of these investigations is the technical staff's wide-ranging expertise and its ability to stay current with new developments. This expertise is enhanced by a research program aimed at dealing with the many problems associated with rapidly evolving space systems. Contributing their capabilities to the research effort are these individual laboratories:

Aerophysics Laboratory: Launch vehicle and reentry fluid mechanics, heat transfer and flight dynamics; chemical and electric propulsion, propellant chemistry, chemical dynamics, environmental chemistry, trace detection; spacecraft structural mechanics, contamination, thermal and structural control; high temperature thermomechanics, gas kinetics and radiation; cw and pulsed chemical and excimer laser development including chemical kinetics, spectroscopy, optical resonators, beam control, atmospheric propagation, laser effects and countermeasures.

Chemistry and Physics Laboratory: Atmospheric chemical reactions, atmospheric optics, light scattering, state-specific chemical reactions and radiative signatures of missile plumes, sensor out-of-field-of-view rejection, applied laser spectroscopy, laser chemistry, laser optoelectronics, solar cell physics, battery electrochemistry, space vacuum and radiation effects on materials, lubrication and surface phenomena, thermionic emission, photosensitive materials and detectors, atomic frequency standards, and environmental chemistry.

Computer Science Laboratory: Program verification, program translation, performance-sensitive system design, distributed architectures for spaceborne computers, fault-tolerant computer systems, artificial intelligence, microelectronics applications, communication protocols, and computer security.

Electronics Research Laboratory: Microelectronics, solid-state device physics, compound semiconductors, radiation hardening; electro-optics, quantum electronics, solid-state lasers, optical propagation and communications; microwave semiconductor devices, microwave/millimeter wave measurements, diagnostics and radiometry, microwave/millimeter wave thermionic devices; atomic time and frequency standards; antennas, rf systems, electromagnetic propagation phenomena, space communication systems.

Materials Sciences Laboratory: Development of new materials: metals, alloys, ceramics, polymers and their composites, and new forms of carbon; nondestructive evaluation, component failure analysis and reliability; fracture mechanics and stress corrosion; analysis and evaluation of materials at cryogenic and elevated temperatures as well as in space and enemy-induced environments.

Space Sciences Laboratory: Magnetospheric, auroral and cosmic ray physics, wave-particle interactions, magnetospheric plasma waves; atmospheric and ionospheric physics, density and composition of the upper atmosphere, remote sensing using atmospheric radiation; solar physics, infrared astronomy, infrared signature analysis; effects of solar activity, magnetic storms and nuclear explosions on the earth's atmosphere, ionosphere and magnetosphere; effects of electromagnetic and particulate radiations on space systems; space instrumentation.